Available online at www.eccomasproceedia.org
Eccomas Proceedia SMART (2023) 1412-1422

ECCOMAS
Proceedia

X ECCOMAS Thematic Conference on Smart Structures and Materials
SMART 2023
D.A. Saravanos, A. Benjeddou, N. Chrysochoidis and T. Theodosiou (Eds)

MAGNETORHEOLOGICAL DAMPERS-BASED CONTROLLABLE INERTER

Jing Cao[1], Donghong Ning[1,*], Shuaishuai Sun[2], Guijie Liu[1], Haiping Du[3]

1. College of Engineering, Ocean University of China, Qingdao, China

2. Department of Precision Machinery and Precision Instrumentation, University of Science and Technology of China, Hefei, China

3. School of Electrical, Computer and Telecommunications Engineering, University of Wollongong, Wollongong, NSW 2522, Australia

Abstract: Inerter has shown advantages in improving vibration control performance, while most studies focus on passive systems. In this paper, a new controllable inerter is proposed based on two magnetorheological (MR) dampers. The proposed inerter includes a new controllable mechanical motion rectifier (CMMR) and a flywheel. The inerter can switch the vibration energy paths by tuning the control currents of MR dampers, and it can convert reciprocating vibration into the rotation of the flywheel. The flywheel can release stored energy to generate controllable force for vibration reduction. The driving energy of the device comes from the mechanical energy in vibration, and the control of reciprocating vibration by CMMR only requires a small amount of electrical energy, which is different from traditional semi-active control. In addition, the frequency domain characteristics of the controllable inerter are analyzed, which shows the inertance of the device can be controlled in a limited frequency band. Based on the system states and ideal force output, a force-tracking algorithm for the device is proposed. Simulation results show that the device can output positive and negative power and effectively achieve better force-tracking performance than traditional variable damping device. This result indicates the feasibility of its application in semi-active vibration control, and it has great potential for practical application.

Key words: Inerter; MR; variable damping; force tracking; vibration control.

© 2023 The Authors. Published by Eccomas Proceedia.
Peer-review under responsibility of the organizing committee of SMART 2023.
doi: 10.7712/150123.9913.451072

1 INTRODUCTION

In 2002, Professor Smith proposed the concept of inerter [1], which is defined as a device with two independent endpoints. The device can produce a reverse force proportional to the relative acceleration of the two ends. According to the analogy of electromechanical systems, the electrical characteristics of resistors, inductors, and capacitors correspond to the mechanical characteristics of damper, spring, and inerter. This concept has promoted the further development of mechanical vibration isolation networks. In recent years, the application of inerter to vibration control has become a popular research topic. Relevant experts and scholars have applied it to various vibration isolation fields: such as motorcycle bogies [2] and aircraft landing gears [3]. Based on its development history, it can be seen that inerter has unique potential for vibration suppression. However, a problem has gradually been discovered: passive inerter can only ensure vibration isolation characteristics within a specific frequency range. Therefore, it is necessary to study variable inerter with continuously adjustable inertance.

Since the discovery of magnetorheological (MR) fluid, researchers have paid attention to its new structure, characteristics, and influence factors [4], [5]. MR can continuously and rapidly change the viscosity of liquid by changing the applied magnetic field intensity. Under the action of the magnetic field, MR can change from a free-flowing liquid to a semi-solid in a few milliseconds, and this change is reversible. This characteristic allows MR dampers to change their damping characteristics in real time [6], [7]. Therefore, MR dampers are widely used in the field of semi-active control [8], [9]. By connecting the variable damping (VD) device and the inerter in series, a variable inerter with continuously adjustable inertance can be obtained, as proposed by Ning [10] through the controllable mechanical motion rectifier (MMR).

Based on the above research, this paper proposes a novel MR dampers-based controllable inerter (MRDCI) by changing the roller clutch in the inerter into MR dampers. By changing the current in the MR dampers, the device can quickly switch the torque and motion transmission direction between the system and the flywheel. MRDCI can store the vibration energy in the flywheel and release the energy through appropriate control strategies. In the process of energy release, the flywheel acts similar to a "motor", thus producing the effect of active control. Since the driving energy comes from the vibration itself, the device only requires a small amount of electrical energy to achieve vibration control of reciprocating motion. Compared with active control, it has great practical application potential. The main contributions of this paper are as follows:

1). MRDCI is proposed and simulated to verify its controllability.

2). Controller is designed to achieve better force tracking performance.

The rest of this paper is organized as follows: Section 2 presents the structure of the controllable inerter and analyses its mechanical characteristics; Section 3 introduces the design of semi-active controller; Section 4 presents the force tracking performance of MRDCI; Finally, the conclusion of this research is given in section 5.

2 DEVICE MODEL

2.1 Description of MRDCI

In the field of vibration control, although active control can theoretically achieve outstanding damping performance, it often results in higher production costs and greater energy consumption. As a result, researchers have focused on developing semi-active control systems that can achieve performance similar to active control systems. With the further development of inerter technology, this idea has become increasingly feasible.

This paper proposes a new design for a semi-active inerter, which is shown in Figure 1. The MRDCI consists of two pairs of rack and pinion (RP) structures connected to the flywheel using two magnetorheological (MR) dampers. The two racks are located on either side of the gear, so the forces they transmit to the top plate are opposite. This means that when the flywheel rotates clockwise or counterclockwise, it can output force in two directions.

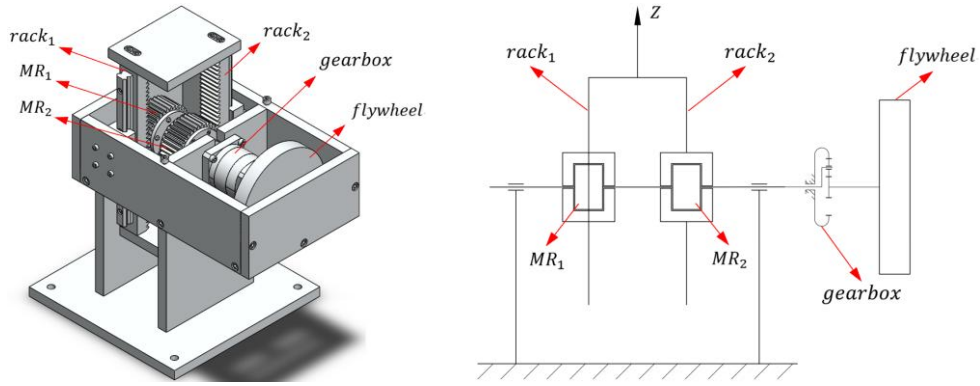

(a). 3D model (b). Simplified model

Figure 1. Controllable inerter design

The function of MRDCI can be explained in more detail in Figure 2. When the flywheel rotates counterclockwise, the left MR damper generates small damping while the other generates large damping. At this point, the flywheel is almost disconnected from rack1, and the torque of the flywheel is mainly transmitted from rack2 to the top plate. As a result, the top plate receives an upward force. When the states of the two MR dampers are switched, the stress direction of the top plate becomes opposite to the previous situation. This means that MRDCI proposed in this paper can control the direction of the flywheel output force.

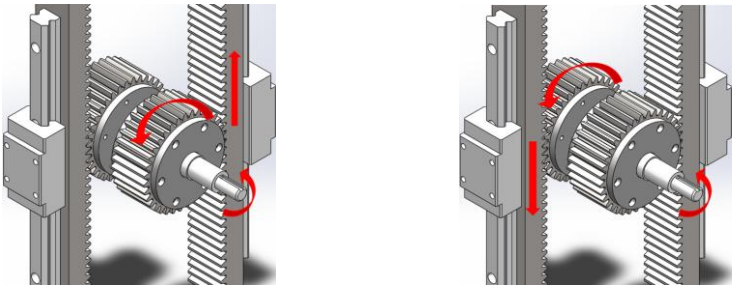

(a). Rack up movement (b). Rack down movement

Figure 2. Controllable inerter working diagram

2.2 System analysis

To better analyse the variable inertance capacity of the system, the torques generated by the MR dampers are simplified, and the dynamic model of the device is established. Let c_1 and $_2$ be the damping constants of the MR dampers, θ_1 be the rotation angle of the flywheel, θ_{mr1} and θ_{mr2} be the angles of the two gears, i be the transmission ratio of the decelerator, j_i be the rotational inertia of the flywheel, r be the radius of both gears, and z be the vertical displacement of the top plate

The torques generated by the two dampers are:

$$\begin{aligned} T_{mr1} &= {}_1(\dot{\theta_{mr1}} - \dot{\theta_1}) \\ T_{mr2} &= {}_2(\dot{\theta_{mr2}} - \dot{\theta_1}) \end{aligned} \tag{1}$$

where $\theta_{mr1} = z/r$, $\theta_{mr2} = -z/r$.

The output force of the device is：

$$F_{out} = F_{mr1} - F_{mr2} = (T_{mr1} - T_{mr2})/r = (c_1 + {}_2)\dot{z}/r - (c_1 - {}_2)\dot{\theta_1} \tag{2}$$

The dynamic model of the flywheel is:

$$ij_i\ddot{\theta_1} = T_{mr1} + T_{mr2} = (c_1 - {}_2)\dot{z}/r - (c_1 + {}_2)\dot{\theta_1} \tag{3}$$

Through Laplace transformation, we have:

$$\frac{\overline{F_{out}}}{\bar{z}s} = \frac{(c_1 + {}_2)}{r^2} - \frac{(c_1 - {}_2)^2}{r^2(c_1 + {}_2 + ij_is)} \tag{4}$$

where $s = j\omega$. According to the above dynamic equation, the admittance of the device can be obtained as follows:

$$Y = \frac{(c_1 + {}_2)}{r^2} - \frac{(c_1 - {}_2)^2(c_1 + {}_2)}{r^2[(c_1 + {}_2)^2 + i^2{j_i}^2\omega^2]} + \frac{(c_1 - {}_2)^2ij_i}{r^2[(c_1 + {}_2)^2 + i^2{j_i}^2\omega^2]}j\omega \tag{5}$$

where $real(Y)$ represents the equivalent damping, and $imag(Y)$ is the equivalent inertance.

The following data are used to simulate the admittance of the system: $i = 7$, $j_i = 30 \times 10^{-4} kgm^2$, $c_{min} = 0.01\ Nms/rad$, $c_{max} = 0.08\ Nms/rad$, and $r = 0.035mm$.

First, when both MR dampers are controlled with the same damping, it can be deduced from equation (6) that the equivalent inertance of the device will always be zero. From Figure 3, it can be seen that the device is equivalent to a VD device.

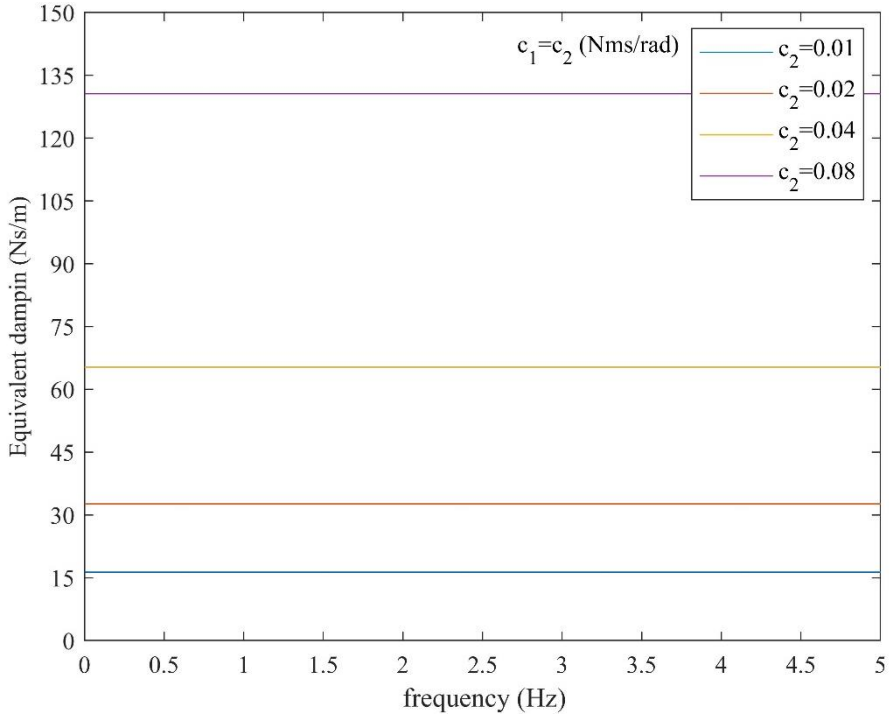

Figure 3. The variable damping capacity

When the c_1 is set to its minimum value, and is varied within its controllable range, as shown in Figure 4, the equivalent inertance of the device can be controlled by c_2.

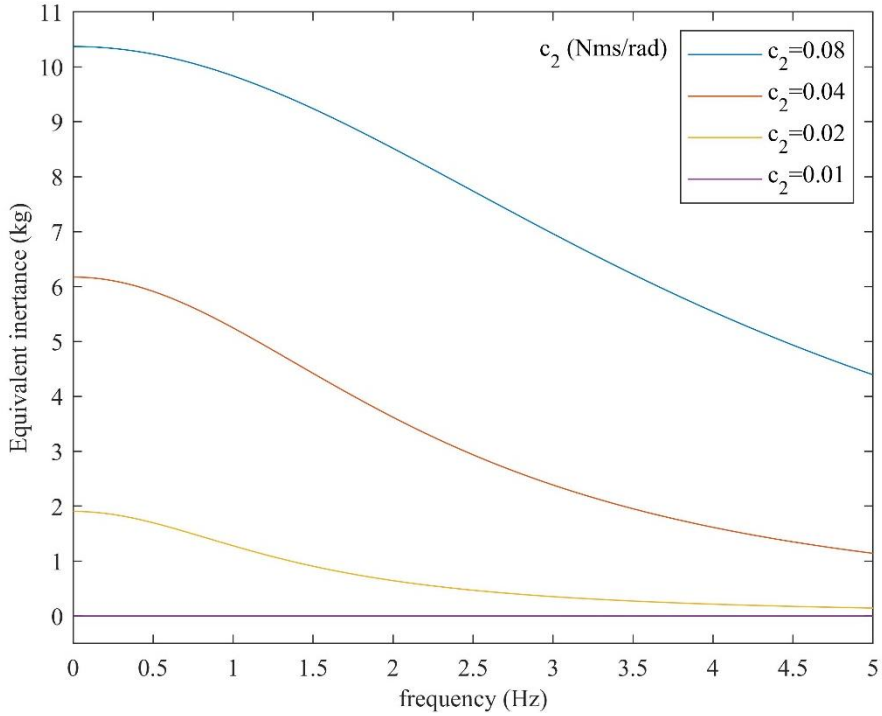

Figure 4. The variable inertance capacity

The admittance analysis indicates that the inertance and damping of the device can be controlled by changing the magnitude of the damping.

3 CONTROLLER DESIGN

3.1 MR damper model

In the previous section, we analyzed the system using linear damping. However, the dynamic characteristics of MR damper are influenced by many factors and exhibit strong nonlinearity. Therefore, it is necessary to establish an accurate MR damper model to describe its characteristics. To facilitate the design of the controller, we select a hyperbolic tangent model [11] to describe the MR damper.

In practical applications, the controller needs to calculate the output torque of the MR dampers by adjusting the output current. The torque output of the two MR dampers is:

$$\begin{gathered} T_{mri} = {}_i\left(\dot{\theta_{mri}} - \dot{\theta_1}\right) + k_i(\theta_{mri} - \theta_1) + \alpha_i z_i + f_i \\ z_i = tanh\left(\beta_i\left(\dot{\theta_{mri}} - \dot{\theta_1}\right) + \delta_i sign(\theta_{mri} - \theta_1)\right) \\ \alpha_i = \alpha_{ai} + \alpha_{bi}u_i \qquad {}_i = {}_{ai} + {}_{bi}u_i \end{gathered} \tag{6}$$

where c_i is the viscosity coefficient, k_i is the stiffness coefficient, α_i is the scale factor of the hysteresis, z is the hysteresis variable given by the hyperbolic tangent function, f_i is the offset of the torque, and u_i is the current of the damper. α_{ai}, α_{bi}, c_{ai}, c_{bi}, β_i, δ_i are parameters that determine the lag model.

Table 1: Parameters of MR dampers

MR damper 1		MR damper 2	
α_{a1}	0.4	α_{a2}	0.4
α_{b1}	10	α_{b2}	10
β_1	20	β	20
δ_1	0.1	δ	0.1
${}_{a1}$	0.008	${}_{a2}$	0.008
${}_{b1}$	0.1	${}_{b2}$	0.1
f_1	0	f	0
k_1	0.02	k	0.02

3.2 Force tracking control

A reasonable control strategy is essential for the whole design. The focus of force tracking control is how to use MRDCI to collect vibration energy and release it at the appropriate time. To achieve this characteristic, the desired force F_{des} is divided into two dampers according to the system state.

Step 1: identify the primary damper for control

Firstly, the force range that can be produced by the two dampers should be defined. When one damper is set to its maximum current (u_{max}) and the other damper is set to its minimum current (0A), the uncontrolled output force and the two limiting values of the output force can be calculated as follows:

$$\begin{aligned} F_{mr0A} &= F_{mr1}(0A) + F_{mr2}(0A) \\ F_{mr1lim} &= F_{mr1}(u_{max}) + F_{mr2}(0A) \\ F_{mr2lim} &= F_{mr1}(0A) + F_{mr2}(u_{max}) \end{aligned} \tag{7}$$

Therefore, the output force range of the two dampers is between $[F_{mr0A}\ F_{mr1lim}]$ and $[F_{mr0A}\ F_{mr2lim}]$, respectively.

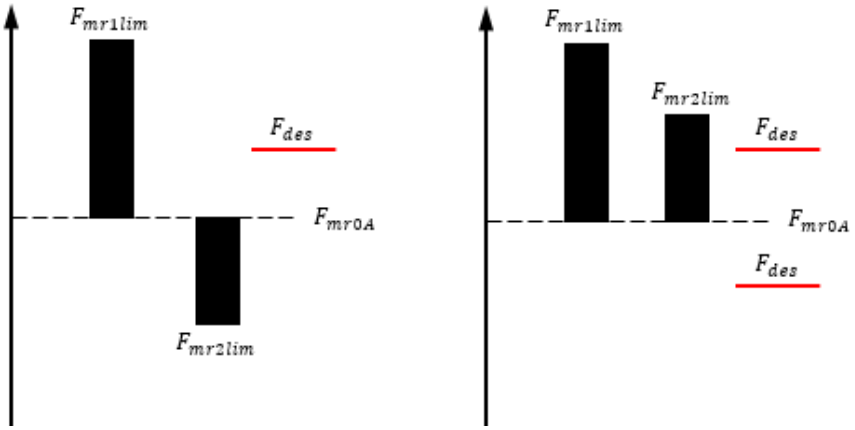

(a) Case one (b) Case two

Figure 5. Force output prediction.

In Figure 5(a), F_{mr1lim} and F_{mr2lim} are located on opposite sides of F_{mr0A}. Therefore, the primary damper for control is determined by the direction of the force limit. However, in Figure 5(b), the limits of the two dampers are on the same side of F_{mr0A}. In this case, to ensure that the flywheel rotates with lower impedance, the damper that makes the rotor and shell rotate in the same direction is chosen as the main damper for control. When F_{des} is on the other side of the limit force, both dampers are set to 0 A current. The realization of the first step is shown in Figure 6, where i represents the main damper for control, j represents another damper, and the three criteria are:

$$\begin{cases} Cn_1 = (F_{mr1lim} - F_{mr0A}) \cdot (F_{mr2lim} - F_{mr0A}) \\ Cn_2 = (F_{mr1lim} - F_{m\,0A}) \cdot (F_{des} - F_{mr0A}) \\ Cn_3 = \dot{\theta}_1 \cdot \dot{\theta}_{mr1} \end{cases} \tag{8}$$

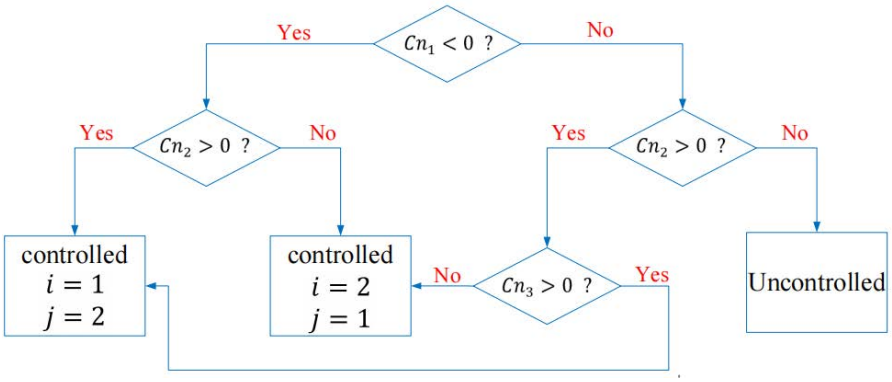

Figure 6. The first step of the control strategy

Step 2: Calculate the force required for each damper

If the device can track the desired force:

$$F_{mrides} = F_{des} - F_{mrj}(0A) \tag{9}$$

If the ultimate force of the primary damper for control is not sufficient to reach the desired force, then another damper is required to assist, as shown below:

$$F_{mrjdes} = F_{des} - F_{mrides} \tag{10}$$

On the contrary, when the primary damper for control is sufficient to reach the desired force, there are:

$$F_{mrjdes} = F_{mrj}(0A) \tag{11}$$

If the device cannot track the desired force, and both dampers cannot reach the desired force, we have:

$$\begin{aligned} F_{mr1des} &= F_{mr1}(0A) \\ F_{mr\ des} &= F_{mr}\ (0A) \end{aligned} \tag{12}$$

Step 3: Calculate the current required by the damper according to the force

According to the hyperbolic tangent model, the relationship between some parameters and current is treated as a linear relationship. The flowchart for solving the current can be obtained based on the Formula 6:

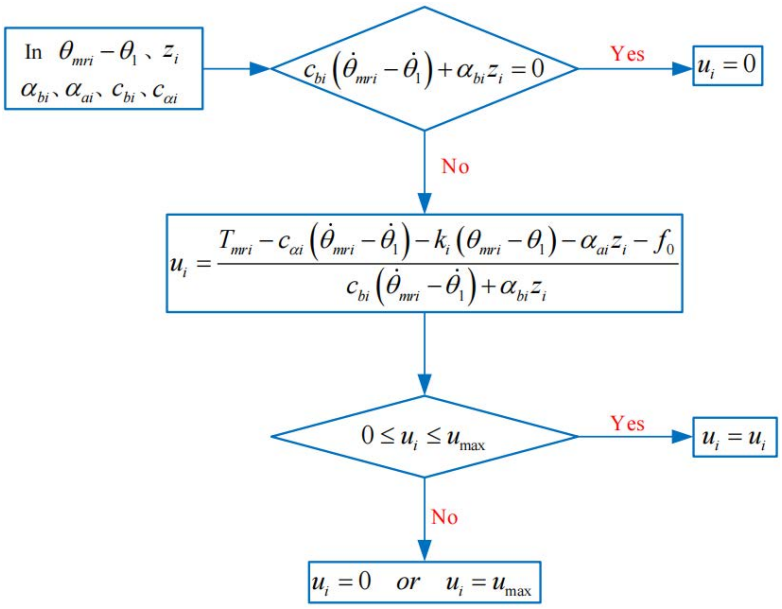

Figure 7. Control current solving process

4 FORCE TRACKING PERFORMANCE OF THE SYSTEM

A sinusoidal excitation $z = 0.01 \cdot sin(4\pi t)$ is applied to the device. The desired force F_{des} is set as a constant. As can be seen from Figure 8, MRDCI has better force tracking performance than a semi-active VD device.

Let t_1 be the time of a sinusoidal excitation period, t_2 be the matching time of MRDCI in one period, and t_3 be the matching time of the semi-active VD device in one period. According to (13), MRDCI has a matching rate that is 13.80% higher than the VD device.

$$\frac{t}{t_1} = 56.88\%$$
$$\frac{t_3}{t_1} = 49.98\% \tag{13}$$

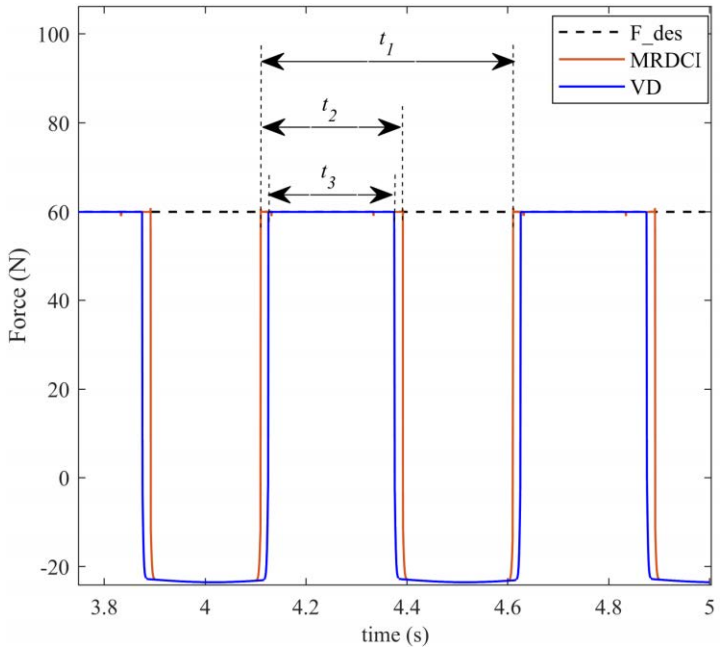

Figure 8. Force tracking performance

When the desired force F_{des} is a random dynamic force, as shown in Figure 9, the working area of MRDCI is divided into four quadrants based on the relationship between the top plate force and displacement. If MRDCI works in the first and third quadrants, it indicates that the flywheel will experience "negative power" and can obtain vibration energy. On the other hand, when MRDCI works in the second and fourth quadrants, it indicates that the flywheel is outputting active force to match the target force. This means that MRDCI can not only consume energy but also store energy in the flywheel for vibration isolation. Consequently, this device exhibits better force tracking performance compared to the VD device.

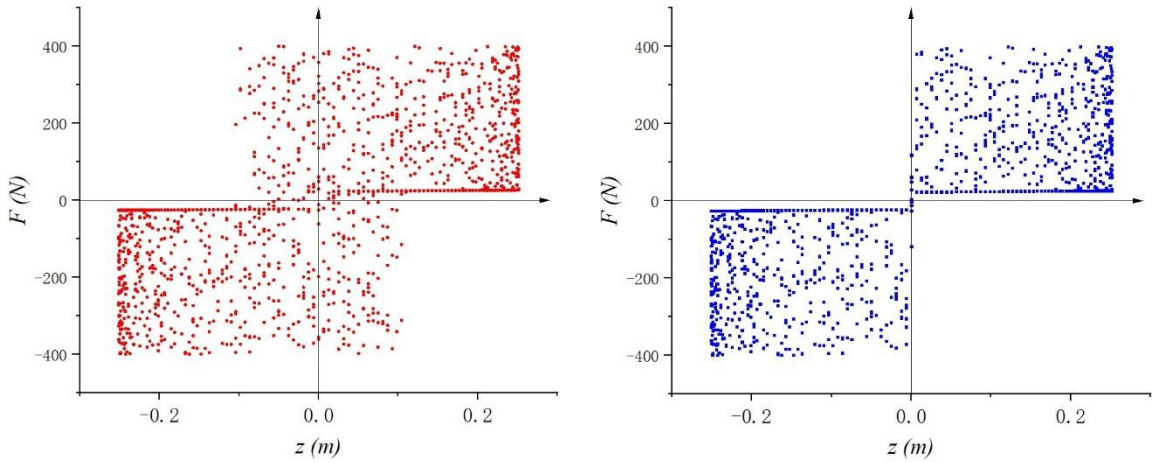

(a) MRDCI (b) VD

Figure 9. Energy flow of the MRDCI and VD

Since the VD device can only control the magnitude of the damping force output, it can only output controllable forces that are opposite to the velocity. As a result, the force direction of the VD device matches the expected direction for only half of the sinusoidal cycle time. Therefore, the matching rate of the VD device under given conditions cannot exceed 50%. By changing different frequencies and amplitudes, Table 1 shows that the proposed controllable inerter device can break through this technical bottleneck.

Table 2: Matching rate under different sinusoidal excitation

sinusoidal excitation		target	MRDCI	VD
frequency (Hz)	amplitude (m)	desired force F_{des} (N)		
2	0.01	60	56.88%	49.98%
	0.02	60	56.08%	49.98%
4	0.01	60	56.12%	49.98%
	0.02	60	54.58%	49.98%
2	0.01	$400 \cdot sin(4\pi t)$	70.06%	47.88%
	0.02	$400 \cdot sin(4\pi t)$	61.60%	47.88%
4	0.01	$400 \cdot sin(8\pi t)$	58.88%	47.84%
	0.02	$400 \cdot sin(8\pi t)$	56.64%	47.60%

5 CONCLUSIONS

This paper proposes a controllable inerter based on magnetorheological dampers, which exbibits variable inertance characteristics that are verified through frequency domain analysis. The mechanism of flywheel energy storage and release is also revealed. A force tracking algorithm is designed based on the system state and ideal force output and is compared with the VD device. The simulation results show that, under a given sinusoidal excitation test, the force tracking matching rate of MRDCI is 13.80% higher than that of the VD device. Because

the VD device can only control the magnitude of the damping force output, its force direction is opposite to the speed direction. This is the main reason for the performance gap between active and semi-active control in the field of vibration control. By employing a certain control strategy, the flywheel can act as a "motor" to a certain extent, breaking through the technical bottleneck of traditional VD device and allowing the force tracking matching rate to exceed 50%. In future work, we will focus on improving control methods by considering energy collection and vibration control and explore the application of this device prototype in other engineering scenarios.

REFERENCES

[1] Smith, M. C. . "Synthesis of mechanical networks: the inerter." *IEEE TRANSACTIONS ON AUTOMATIC CONTROL AC* (2002).

[2] Papageorgiou, C. , et al. "Experimental testing and modelling of a passive mechanical steering compensator for high-performance motorcycles." (2007).

[3] DONG, et al. "Application of Inerter to Aircraft Landing Gear Suspension." *IEEE*.

[4] Jedryczka, C. , P. Sujka , and W. Szelag . "The influence of magnetic hysteresis on magnetorheological fluid clutch operation." *Compel International Journal for Computation & Mathematics in Electrical & Electronic Engineering* 28.3(2009):págs. 711-721.

[5] Wang, N. , et al. "Microscopic characteristics of magnetorheological fluids subjected to magnetic fields." *Journal of magnetism and magnetic materials* 501.May(2020):166443.1-166443.11.

[6] Qian, et al. "A magnetorheological fluid mount featuring squeeze mode: analysis and testing." *Smart Materials & Structures* (2016).

[7] Bai, Xcs . "Controllability of magnetorheological shock absorber: II. Testing and analysis." *Smart Materials & Structures* 28.1(2019).

[8] Ning, D. , et al. "Integrated active and semi-active control for seat suspension of a heavy duty vehicle:." *SAGE PublicationsSage UK: London, England* 1(2017).

[9] Liu, Xinhua , et al. "A new AI-surrogate model for dynamics analysis of a magnetorheological damper in the semi-active seat suspension." *Smart Materials and Structures* 29.3(2020).

[10] [1] Ning, D. , et al. "An electromagnetic variable inertance device for seat suspension vibration control." *Mechanical Systems and Signal Processing* 133(2019):106259-.

[11] Kwok, N. M. , et al. "A novel hysteretic model for magnetorheological fluid dampers and parameter identification using particle swarm optimization." *Sensors & Actuators A Physical* 132.2(2006):441-451.